Splitting of the zero-energy edge states in bilayer graphene

Matheus P. Lima,[1,*] Antônio J. R. da Silva,[1,2,†] and A. Fazzio[1,3,‡]
[1]*Instituto de Física, Universidade de São Paulo, CP 66318, 05315-970 São Paulo, SP, Brazil*
[2]*Laboratorio Nacional de Luz Síncrotron (LNLS), CP 6192, 13083-970 Campinas, SP, Brazil*
[3]*Centro de Ciências Naturais e Humanas, Universidade Federal do ABC, 09210-170 Santo André, SP, Brazil*
(Received 2 October 2009; revised manuscript received 28 December 2009; published 28 January 2010)

Bilayer graphene nanoribbons with zigzag termination are studied within the tight-binding model. We also include single-site electron-electron interactions via the Hubbard model within the unrestricted Hartree-Fock approach. We show that either the interactions between the outermost edge atoms or the presence of a magnetic order can cause a splitting of the zero-energy edge states. Two kinds of edge alignments are considered. For one kind of edge alignment (α) the system is nonmagnetic unless the Hubbard parameter U becomes greater than a critical value U_c. For the other kind of edge alignment (β) the system is magnetic for any $U>0$. Our results agree very well with *ab initio* density functional theory calculations.

DOI: 10.1103/PhysRevB.81.045430 PACS number(s): 73.22.−f, 72.80.Rj, 61.48.De, 71.15.Nc

I. INTRODUCTION

Great efforts have been made in the last decade aiming at employing new materials as electronic devices.[1–3] This need is due to several factors, among which we mention the limitations of silicon-based devices[4,5] and the challenge of spintronics.[6,7] In this scenario, the graphene[8] emerges as a most promising material, because of its unique properties. Measurements of massless fermions with high mobility[9,10] and Quantum Hall effect[11,12] are examples of the special characteristics of this material.

The graphene in its pristine configuration is a gapless material. Thus, having in mind possible device applications, it is interesting to be able to open and control a gap. One possibility is cutting the graphene in order to create a lateral quantum confinement, synthesizing the so-called "graphene nanoribbons" (GNRs).[13,14] This quasi-one-dimensional material possesses a gap that varies with the width, and *sub*-10 nm widths are required for a large enough gap to enable room-temperature applications. Depending on the cutting direction, GNRs can be formed with two different edge shapes, namely zigzag or armchair. The electronic structure and the magnetic properties of this material strongly depend on the shape of the edge termination. Theoretical works predict that when the graphene is cut forming GNRs with a zigzag termination, a large density-of-states (DOS) peak occurs at the Fermi level. This is mainly composed by half-filled states, which is unstable, leading to the appearance of a magnetized state (ferromagnetic or antiferromagnetic) with lower energy. The decrease of the total energy occurs because the half-filled DOS peak is broken down into two peaks: one with energy lower than the Fermi level, composed by full-filled states, and another with energy higher than Fermi level, composed by unoccupied states. In other words, the nonmagnetic GNRs with zigzag termination have an electronic instability that can be resolved with the appearance of a magnetic order, that splits the half-filled edge states, and that eliminates the large DOS peak at the Fermi energy. The presence of strongly localized states near the edges, which are investigated both theoretically[15] and experimentally,[16,17] is fundamental to explain the appearance of this magnetism, in the sense that it is the localization of the wave function that allows a local magnetic moment. So, the electronic stability of GNRs with zigzag termination can be linked to the splitting of the edge states caused by the presence of an edge magnetism.

Recently it was observed that by stacking two layers of graphene, forming a "bilayer graphene," a new mechanism of control of the gap is possible.[18–20] In fact, the charge transfer between the layers will affect the band structure and is a suitable mechanism to control the electronic structure of graphene derived materials. Another advantage of bilayer graphene is the low $1/f$ noise,[21] when compared to a single layer. This occurs because two stacked layers are less sensitive to external perturbations than an isolated one, and therefore will be more suitable for device applications.

Combining the lateral quantum confinement with the stacking of two layers, bilayer graphene nanoribbons (BGNRs) can be constructed, a system that possesses sufficient ingredients to make graphene-based nanoelectronic devices. The fabrication of a transistor using BGNR with widths of the order of 2 nm (Ref. 22) has been recently reported. The edge termination of the BGNRs (as well as GNRs) is strongly relevant for the electronic structure of this material.[23–25] Theoretical investigations, within the tight-binding approach, predict that the BGNRs with a zigzag termination (B-ZGNRs) also possesses half-filled strong localized edge states with zero energy[26] and, as a result, a large DOS peak at the Fermi level also occurs. Thus, a magnetic ordering can emerge to stabilize the system. However, the B-ZGNRs possess two kinds of edge alignments, illustrated in Fig. 1. In (a) the α alignment is presented, and in (b) the β alignment is presented. First-principles simulations predict that the α alignment is energetically favorable and have a zero magnetic moment, whereas the β alignment have a nonzero magnetic moment.[24] At the α alignment there is a situation that differs qualitatively from the β alignment and the GNRs, because the stability is not associated with an edge magnetism. We show in this paper that the mechanism that mainly stabilizes the B-ZGNRs at the α alignment is the interaction between the outermost carbon atoms of the two layers, whereas the stability at the β alignment is associated solely to an edge magnetism.

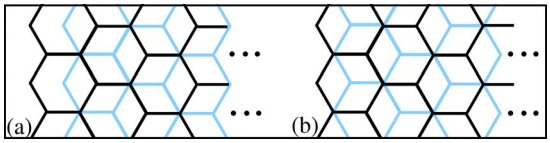

FIG. 1. (Color online) We consider two edge alignments for the bilayer graphene (a) α alignment, where the outermost C edge atoms possess only one C nearest neighbor at the other layer. (b) β alignment, where the outermost C edge atoms possesses three C nearest neighbors at the other layer. The dark and gray (blue) layers are the upper and bottom ones.

We present in this paper a detailed discussion of the magnetism and electronic structure of B-ZGNR using a tight-binding approach.[27–29] The absence of a magnetic order in B-ZGNRs with an α alignment[24] is completely explained by the inclusion of a weak interaction between the edge atoms of the two layers with a hopping t_{edge} [see Fig. 2(c)] that splits the half-filled states, and stabilizes the system. Considering the single-site electron repulsion via a Hubbard model, within the unrestricted Hartree-Fock approximation,[30] we found that B-ZGNRs at the α alignment will be nonmagnetic unless $U > U_c$ and B-ZGNRs at the β alignment will be magnetic for any value of U. This behavior depends solely on the splitting of the edge states, which are the four energy bands around the Fermi level for $2\pi/3 < |k| < \pi$. We show this with analytical arguments, by calculating the zero-energy wave functions of the edge states for both α and β alignments at the regime $U=0$ and $t_{edge}=0$, and we use first-order perturbation theory to calculate the local magnetization and the energy bands of the edge states when $t_{edge}>0$ and $U>0$. We corroborate these results with a numerical solution of this Hamiltonian, and compare with state-of-the-art *ab initio simulations*.[24]

II. METHODOLOGY

The Hamiltonian we use to describe the B-ZGNR is given by

$$H = H_1 + H_2 + H_{1,2} + H_U + H_{edge}. \tag{1}$$

The H_i with $i=1$ or 2 are the single layer Hamiltonians written as

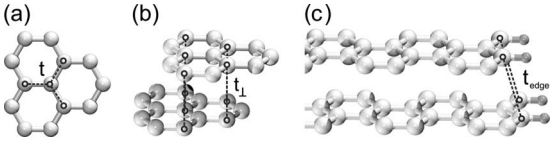

FIG. 2. An illustration of the hopping interactions considered in the present work. In (a) we show the in-layer first neighbor hopping t. In (b) we show the interlayer bulk interactions $t_\perp$. In (c) we show the interlayer edge interactions t_{edge}. The last one is considered only between the edge atoms localized at the B-ZGNR border. In (c), the edge atoms are saturated with hydrogen to indicate the bilayer border.

$$H_i = -t\sum_{\sigma}\sum_{m,n} a^{\dagger}_{i,\sigma}(m,n)[b_{i,\sigma}(m,n) + b_{i,\sigma}(m-1,n) + b_{i,\sigma}(m,n-1)] + \text{H.c.}, \tag{2}$$

where, t is the in-layer first neighbor hopping [see Fig. 2(a)], $a_{i,\sigma}(m,n)$ and $b_{i,\sigma}(m,n)$ [$a^{\dagger}_{i,\sigma}(m,n)$ and $b^{\dagger}_{i,\sigma}(m,n)$] annihilates (creates) a π electron with spin σ at the site (m,n) at the sublattice A or B, respectively. The m index of the sites is related to the periodic direction along the nanoribbons growth direction, and may assume any integer value in the interval $(-\infty,\infty)$. On the other hand, the n index is associated with the lateral direction, and a lateral quantum confinement can be employed limiting n to the interval $[0,N-1]$. Since graphene possesses two atoms in the unit cell, this represents a nanoribbon containing $2N$ C atoms from one edge to the other.

The term $H_{1,2}$ contains the bulk interactions between the two layers. We consider that only the atoms of one layer that are positioned exactly above an atom of the other layer interact with a hopping $t_\perp$ [see Fig. 2(b)]. The layers are stacked at the Bernal pattern, what means that the A-sublattice of one layer interacts with the B sublattice of the other layer. However, the kind of edge alignment must be considered. At the β alignment, all sites of the A sublattice of one layer interact with some site of the B sublattice of the other layer. In this case, the bulk interaction term can be written as

$$H^{\beta}_{1,2} = -t_\perp \sum_{\sigma,m,n} a^{\dagger}_{1,\sigma}(m,n) b_{2,\sigma}(m,n) + \text{H.c.} \tag{3}$$

At the α alignment, the outermost sites of the sublattices A and B do not have any C atom of the other layer exactly above (or below) them. The interaction term can be written as

$$H^{\alpha}_{1,2} = -t_\perp \sum_{\sigma,m}\sum_{n=1}^{N-1} a^{\dagger}_{1,\sigma}(m,n) b_{2,\sigma}(m,n-1) + \text{H.c.} \tag{4}$$

In order to describe the magnetic properties, we include the single-site electron repulsion energy via Hubbard model, given by

$$E_U = U\sum_{i,m,n}\sum_{c=a,b}\left(n^c_{i,\uparrow}(m,n) - \frac{1}{2}\right)\left(n^c_{i,\downarrow}(m,n) - \frac{1}{2}\right), \tag{5}$$

where U is the Hubbard parameter, and $n^c_{i,\uparrow}(m,n) = c^{\dagger}_{i,\sigma}(m,n)c_{i,\sigma}(m,n)$ is the number operator with $c=a$ or b. The factors $-1/2$ inside the brackets are included uniquely to conveniently define the energy zero. Within the Unrestricted Hartree-Fock approach, the single-site electron repulsion contribution to the Hamiltonian is

$$H_U = U\sum_{i,\sigma,m,n}\left[\left(\langle n^a_{i,-\sigma}(m,n)\rangle - \frac{1}{2}\right)a^{\dagger}_{i,\sigma}(m,n)a_{i,\sigma}(m,n) + \left(\langle n^b_{i,-\sigma}(m,n)\rangle - \frac{1}{2}\right)b^{\dagger}_{i,\sigma}(m,n)b_{i,\sigma}(m,n)\right], \tag{6}$$

where, $\langle n^a_{i,\sigma}(m,n)\rangle(\langle n^b_{i,\sigma}(m,n)\rangle)$ is the density of electrons

with spin σ, at the site (m,n) at the A sublattice (B sublattice) of layer i.

If solely the terms H_i, $H_{1,2}$, and H_U are considered, the conclusion is that the magnetism is the only way to split the zero-energy states.[26] As already mentioned, these conclusions do not agree with the *ab initio* simulations, which predict that for the α alignment the splitting of the edge states can occur even without the presence of a magnetic order. This paper will show that the interaction between the edge atoms, associated with the kind of edge alignment, have a strong relevance to the presence or absence of magnetic moment, and to the splitting of the half-filled zero-energy edge states, contributing to the electronic stabilization of the system. In order to consider these edge interactions, we explicitly include the term H_{edge} that contains only the interaction between the outermost C atoms of one layer with the outermost C atoms of the other layer with a small hopping t_{edge} [see Fig. 2(c)]. The edge alignment must also be considered, and for the α alignment, we have

$$H_{edge}^{\alpha} = -t_{edge}\sum_{\sigma,m}[a_{1,\sigma}^{\dagger}(m,0)a_{2,\sigma}(m,0) + b_{1,\sigma}^{\dagger}(m,N-1)b_{2,\sigma}(m,N-1)] + \text{H.c.}, \tag{7}$$

whereas, for the β alignment, we have:

$$H_{edge}^{\beta} = -t_{edge}\sum_{\sigma,m}[a_{1,\sigma}^{\dagger}(m,0)(a_{2,\sigma}(m,0) + a_{2,\sigma}(m+1,0)) + b_{1,\sigma}^{\dagger}(m,N-1)(b_{2,\sigma}(m,N-1) + b_{2,\sigma}(m+1,N-1))] + \text{H.c.} \tag{8}$$

In our calculations, we guarantee the periodicity by making use of the Bloch theorem. Therefore, we use the following unitary transformations:

$$a_{i,\sigma}(k,n) = \frac{1}{\sqrt{N}}\sum_{m} e^{ikm}a_{i,\sigma}(m,n), \tag{9}$$

$$b_{i,\sigma}(k,n) = \frac{1}{\sqrt{N}}\sum_{m} e^{ikm}b_{i,\sigma}(m,n), \tag{10}$$

where $k \in [-\pi,\pi]$ is the crystal moment. Thus, inverting the above expression and substituting the operators $a_{i,\sigma}(m,n)$ and $b_{i,\sigma}(m,n)$ in each term of Eq. (1), the Hamiltonian can be written as a sum of k-dependent terms ($H=\Sigma_k H(k)$).

The k-dependent Hamiltonian for a single layer is

$$H_i(k) = -t\sum_{i,\sigma}\sum_{n} a_{i,\sigma}^{\dagger}(k,n)[b_{i,\sigma}(k,n)(1+e^{ik}) + b_{i,\sigma}(k,n-1)] + \text{H.c.} \tag{11}$$

For the interlayer interaction, we find for the β alignment

$$H_{1,2}^{\beta}(k) = -t_{\perp}\sum_{\sigma,n} a_{1,\sigma}^{\dagger}(k,n)b_{2,\sigma}(k,n) + \text{H.c.} \tag{12}$$

and for the α alignment

$$H_{1,2}^{\alpha}(k) = -t_{\perp}\sum_{\sigma}\sum_{n=1}^{N-1} a_{1,\sigma}^{\dagger}(k,n)b_{2,\sigma}(k,n-1) + \text{H.c.} \tag{13}$$

The k-dependent electron repulsion mean-field term is

$$H_U(k) = U\sum_{i,\sigma,n}\left[\left(\langle n_{i,-\sigma}^{a}(n)\rangle - \frac{1}{2}\right)a_{i,\sigma}^{\dagger}(k,n)a_{i,\sigma}(k,n) + \left(\langle n_{i,-\sigma}^{b}(n)\rangle - \frac{1}{2}\right)b_{i,\sigma}^{\dagger}(k,n)b_{i,\sigma}(k,n)\right], \tag{14}$$

where the charge density is given by

$$\langle n_{i,\sigma}^{a}(n)\rangle = \frac{1}{2\pi}\int_{-\pi}^{\pi} dk\langle a_{i,\sigma}^{\dagger}(k,n)a_{i,\sigma}(k,n)\rangle, \tag{15}$$

$$\langle n_{i,\sigma}^{b}(n)\rangle = \frac{1}{2\pi}\int_{-\pi}^{\pi} dk\langle b_{i,\sigma}^{\dagger}(k,n)b_{i,\sigma}(k,n)\rangle. \tag{16}$$

Finally, the k-dependent edge interactions for the α alignment are

$$H_{edge}^{\alpha}(k) = -t_{edge}\sum_{\sigma}[a_{1,\sigma}^{\dagger}(k,0)a_{2,\sigma}(k,0) + b_{1,\sigma}^{\dagger}(k,N-1)b_{2,\sigma}(k,N-1)] + \text{H.c.} \tag{17}$$

and for the β alignment

$$H_{edge}^{\beta}(k) = -t_{edge}\sum_{\sigma}[(1+e^{-ik})a_{1,\sigma}^{\dagger}(k,0)a_{2,\sigma}(k,0) + (1+e^{-ik})b_{1,\sigma}^{\dagger}(k,N-1)b_{2,\sigma}(k,N-1)] + \text{H.c.} \tag{18}$$

When the single-site electron repulsion H_U is considered, the numerical calculations are performed with a self-consistent-field (SCF) convergence. Employing different initial densities at the beginning of the SCF cycle it is possible to obtain different converged densities. We find that the converged densities possesses a local magnetic moment only near the edge sites; i.e., the density of the $\uparrow$ electrons greatly differs from the densities of the $\downarrow$ electrons only near the outermost sites.

III. RESULTS

A. Analytical analysis

In this section, we will discuss the edge states for the α and the β alignments. It will be presented the expressions for the wave functions for the special regime where $U=t_{edge}=0$ for both α and β alignments. For this regime, the edge states are half-filled zero-energy states, and can be calculated analytically. After this, it will be calculated the splitting of these zero-energy levels in the regime $U>0$ and $t_{edge}>0$ through first-order perturbation theory. It will be shown how the energy bands for the edge states depend on the edge alignment (α or β) when $U>0$ and $t_{edge}>0$.

The general form of the eigenstates for $U=0$ is given by

$$|\psi,k\rangle = \sum_n \sum_{i=1}^{2} [\gamma_i(k,n)|a,i,k,n\rangle + \lambda_i(k,n)|b,i,k,n\rangle], \quad (19)$$

where $|c,i,k,n\rangle = c_i^{\dagger}(k,n)|0\rangle$ for $c=a$ or b, are the single-electron basis vectors we use. The spin index σ can be suppressed. $\gamma_i(k,n)$ and $\lambda_i(k,n)$ are the coefficients that multiply each basis vector $|c,i,k,n\rangle$. In order to find the wave functions for the edge states, the methodology presented in Ref. 26 is followed. The Hamiltonian of Eq. (1) is applied to the eigenstates of Eq. (19) and is equaled to zero. For the B-ZGNRs at the α alignment with $t_{edge}=U=0$, we found the following relations:

$$\begin{bmatrix} \gamma_1(k,n+1) \\ \gamma_2(k,n+1) \end{bmatrix} = e^{-ik/2} D_k \begin{bmatrix} 1 & 0 \\ -\frac{t_\perp}{t} & 1 \end{bmatrix} \begin{bmatrix} \gamma_1(k,n) \\ \gamma_2(k,n) \end{bmatrix}, \quad (20)$$

with $D_k=-2\cos(\frac{k}{2})$. Observing that

$$\begin{bmatrix} 1 & 0 \\ -\frac{t_\perp}{t} & 1 \end{bmatrix}^n = \begin{bmatrix} 1 & 0 \\ -n\frac{t_\perp}{t} & 1 \end{bmatrix}, \quad (21)$$

it is easy to show that

$$\begin{bmatrix} \gamma_1(k,n) \\ \gamma_2(k,n) \end{bmatrix} = e^{-ik/2n} D_k^n \begin{bmatrix} 1 & 0 \\ -n\frac{t_\perp}{t} & 1 \end{bmatrix} \begin{bmatrix} \gamma_1(k,0) \\ \gamma_2(k,0) \end{bmatrix}. \quad (22)$$

The above relation involves a 2×2 matrix, which means that two degenerated wave functions with zero energy can be found with this relation. For any two linearly independent choices of $\gamma_1(k,0)$ and $\gamma_2(k,0)$, two degenerated wave functions can be calculated. Therefore, we found one wave function choosing $\gamma_1(k,0)=1$ and $\gamma_2(k,0)=0$, leading to a eigenstate with the coefficients given by

$$\gamma_1^1(k,n) = C_1^{\alpha}(k) e^{-ik/2n} D_k^n,$$

$$\gamma_2^1(k,n) = -C_1^{\alpha}(k) e^{-ik/2n} D_k^n n\frac{t_\perp}{t}. \quad (23)$$

We found another eigenstate choosing $\gamma_1(k,0)=0$ and $\gamma_2(k,0)=1$, leading to a wave function with the coefficients given by

$$\gamma_1^2(k,n) = 0,$$

$$\gamma_2^2(k,n) = C_2^{\alpha}(k) e^{-ik/2n} D_k^n. \quad (24)$$

Note that two coefficients $[\gamma_1^{1,2}(k,n)$ and $\gamma_2^{1,2}(k,n)]$ are necessary to define a state with a crystal moment k, and their subscripts are related to the layer label (1 or 2). $C_1^{\alpha}(k)$ and $C_2^{\alpha}(k)$ are the normalization constants for each k, and the superscript α is related to the kind of edge alignment. Considering a semi-infinite bilayer graphene, these normalization constants are different from zero only when $|D_k|<1$. This means that the edge states possess zero energy only when $-\pi<k<-\frac{2\pi}{3}$ and $\frac{2\pi}{3}<k<\pi$. The state given by Eq. (23) is not orthogonal to the state of Eq. (24). Orthogonalizing Eq. (23) with respect to Eq. (24) we obtain

$$\gamma_1^1(k,n) = C_1^{\alpha}(k) e^{-ik/2n} D_k^n$$

$$\gamma_2^1(k,n) = -C_1^{\alpha}(k) e^{-ik/2n} D_k^n \frac{t_\perp}{t}\left(n - \frac{D_k^2}{1-D_k^2}\right). \quad (25)$$

The normalization factor for Eq. (25) is $|C_1^{\alpha}(k)|^2=(1-D_k^2)^3/[(t_\perp/t)^2 D_k^2+(1-D_k^2)^2]$ and for Eq. (24) is $|C_2^{\alpha}(k)|=(1-D_k^2)$. These wave functions survive only near the site $n=0$, therefore we can say that these wave functions are localized near the edges indexed by $n=0$.

Applying the Hamiltonian of Eq. (1) to the eigenstate of Eq. (19) we also found an expression for the $\lambda_i(k,n)$ that is analogous to Eq. (22). This relation will give two more degenerated wave functions, but with the particular feature that those are localized at the other side of the B-ZGNR when compared to the wave functions of Eqs. (24) and (25). Replacing $\gamma_i(k,n)$ by $\lambda_i(k,n)$ and n by $N-n-1$ and taking the complex conjugate of Eqs. (24) and (25), we obtain these other edge states. Thus, there are four zero-energy edge states, associated with the four edges of the B-ZGNR. We also point out that the coefficients $\gamma_i(k,n)$ do not depends on the coefficient $\lambda_i(k,n)$, and vice versa.

Up to this point, we have calculated the edge states for the B-ZGNRs at the α alignment using the methodology of Ref. 26, where those for the β alignment were calculated, and are given by

$$\gamma_1^1(k,n) = C_1^{\beta}(k) e^{-ik/2n} D_k^n$$

$$\gamma_2^1(k,n) = -C_1^{\beta}(k) e^{-ik/2(n-1)} D_k^{n-1} \frac{t_\perp}{t}\left(n - \frac{D_k^2}{1-D_k^2}\right), \quad (26)$$

and

$$\gamma_1^2(k,n) = 0,$$

$$\gamma_2^2(k,n) = C_2^{\beta}(k) e^{-ik/2n} D_k^n t, \quad (27)$$

with $|C_1^{\beta}(k)|^2=(1-D_k^2)^3/[(t_\perp/t)^2+(1-D_k^2)^2]$ and $|C_2^{\beta}(k)|=(1-D_k^2)$.

The two differences between the wave functions for the α and β alignments are only a factor of $e^{ik/2}/D_k$ for $\gamma_2^1(k,n)$ and the normalization constant $C_1(k)$. In particular, when $k=\pi$ (K symmetry point), the α alignment presents two wave functions strictly localized at the outermost edge atoms, whereas the β alignment presents one wave function strictly localized and another with nonzero coefficient for $n=0$ in one layer, and $n=1$ in the other layer.

In order to see the difference between these two alignments when a local magnetization is present, let us consider the electron repulsion in the form of Eq. (14). However, we will impose that only the edge atoms indexed by $n=0$ belonging to the A sublattice have a small magnetic polarization, i.e., $\langle n_{i,\uparrow}^a(n=0)\rangle=\frac{1}{2}+\delta$, $\langle n_{i,\downarrow}^a(n=0)\rangle=\frac{1}{2}-\delta$, and, the density at all other sites "n", for each spin channel, is $\frac{1}{2}$. This will be a suitable approach, since a numerical solution with the inclusion of the single-site electron repulsion combined

with a SCF convergence leads to a state where the local magnetization at the edge atoms are much more pronounced than at the other atoms.[31,32] This happens because the presence of the edges introduces surface (edge) states that are highly localized and with an energy band with very small dispersion around the Fermi level. In other words, as opposed to the bulk where a large band dispersion prevents that the value of U leads to the development of local magnetic moments,[33] at the edges the ratio U/t is such that there occurs the appearance of such moments.

With this approach, Eq. (14) reduces to

$$H_U(k) = U\sum_{i,\sigma}[-sgn(\sigma)\delta a^{\dagger}_{i,\sigma}(k,0)a_{i,\sigma}(k,0)] + \text{H.c.}, \quad (28)$$

with $\text{sgn}(\uparrow)=+1$ and $\text{sgn}(\downarrow)=-1$.

The inclusion of $H_U(k)$ causes a splitting $\Delta_U(k)$ of the zero-energy states, that can be calculated through first-order perturbation theory, with the expression $\Delta_U=\langle\psi|H_U|\psi\rangle$.

For the α alignment, the zero-energy states defined by Eq. (25) split as

$$\Delta_U^{1,\alpha}(k) = -\,\text{sgn}(\sigma)U\delta|C_1^{\alpha}(k)|^2\left[1+\frac{t_{\perp}^2}{t^2}\frac{D_k^4}{(1-D_k^2)^2}\right], \quad (29)$$

and, for the β alignment, the equivalent states, defined by Eq. (26) split as

$$\Delta_U^{1,\beta}(k) = -\,\text{sgn}(\sigma)U\delta|C_1^{\beta}(k)|^2\left[1+\frac{t_{\perp}^2}{t^2}\frac{D_k^2}{(1-D_k^2)^2}\right]. \quad (30)$$

For both α and β alignments, the splitting of the other edge states, defined in Eqs. (24) and (27), respectively, is exactly the same, and given by

$$\Delta_U^{2,\alpha;\beta}(k) = -\,\text{sgn}(\sigma)U\delta|C_2(k)|^2, \quad (31)$$

with $|C_2^{\alpha}(k)|^2=|C_2^{\beta}(k)|^2\equiv|C_2(k)|^2$.

The resultant splitting due to an antiferromagnetic ordering between the edges can also be calculated replacing δ by $(-1)^i\delta$ in expression (28), where i is the layer index. In Fig. 3 we present the splitting of the zero-energy levels for the α and β alignments, for both the ferromagnetic (F) as well as the antiferromagnetic (AF) ordering. Figure 3(a) presents the $\Delta_U^1(k)$ for the F ordering and (b) presents the $\Delta_U^1(k)$ for the AF. Finally, (c) and (d) present the $\Delta_U^2(k)$ for the F and AF, respectively. $\Delta_U^{1,\alpha}(k)$ and $\Delta_U^{1,\beta}(k)$ have only very small differences. Moreover, $\Delta_U^{2,\alpha}(k)$ coincide for both edge alignments, which is a consequence of the equality of their wave functions. Therefore, the behavior of the α-B-ZGNR and β-B-ZGNR is very similar if only a magnetic perturbation is considered.

At the first Brillouin-zone border ($k=\pi$), the magnitude of the magnetic splitting can be calculated with expressions (29)–(31). This splitting is exactly $U\delta$ for the wave functions presented in Eqs. (24), (25), and (27). Moreover, for the wave functions presented in Eq. (26), the splitting at $k=\pi$ is smaller, and depends on $t/t_{\perp}$.

From the expressions presented in Eqs. (29)–(31), it can also be inferred that the $\uparrow$ states suffer a positive splitting, whereas the $\downarrow$ states suffer a negative splitting (or vice versa, depending on the signal of the local magnetic moment at the edge atoms). This fact imposes a peculiar electron-hole symmetry, where the occupied states with spin σ are symmetric with respect to the unoccupied states with spin $-\sigma$, and vice versa. This can be observed in Fig. 3.

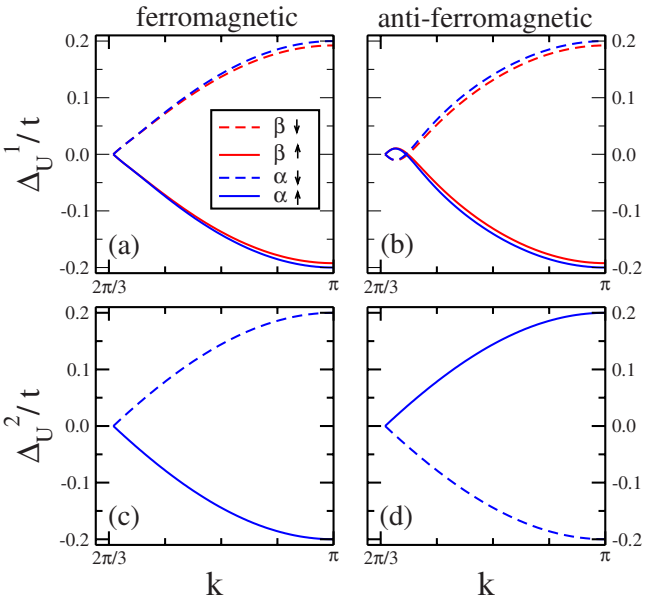

FIG. 3. (Color online) The splitting $\Delta_U^1(k)$ for both α and β alignments is presented. In (a) the ferromagnetic case is presented, and in (b) the antiferromagnetic case is presented. The splitting $\Delta_U^2(k)$ is also presented. In (c) the ferromagnetic order is presented, and in (d) the antiferromagnetic order is presented. We use $U=t$, $\delta=0.2$, and $t_{\perp}=0.2t$.

Now, we focus at the edge atoms interactions in the regime $U=0$ and $t_{edge}>0$. For the β alignment, the term in the Hamiltonian that includes the interlayer edge atoms interactions [Eq. (18)] reduces to zero at the K symmetry point. This means that inclusion of such interaction does not split the edge states at the first Brillouin-zone border, where the edge wave functions are strictly localized. First-principles calculations reveal that a repulsive interaction between the edges occurs for this kind of alignment.[24] Therefore, for a realistic situation the distance between the edge atoms considerably increases and the t_{edge} can be neglected. Because of these arguments, we will not consider in this work the interaction between edge atoms for the β alignment.

However, for the α alignment there is a completely different scenario. The edge interactions are responsible for the splitting of the edge states, including the K symmetry point. First-principles calculations predict the existence of a chemical bond between the edge atoms of the two layers, which causes an edge attraction for this alignment.[24] Because the value of t_{edge} have a close relationship with the distance between the edge atoms, the edge interaction term H_{edge} *must* be considered for this alignment. To better understand the effect of the edge interactions for the α alignment, it is interesting initially to investigate the regime $t_{edge}>0$ and $U=0$.

As already done for the Hubbard term, the splitting of the zero-energy edge states due to the inclusion of the edge interactions can be calculated using First Order Perturbation Theory. To do this, it is important to observe that the edge

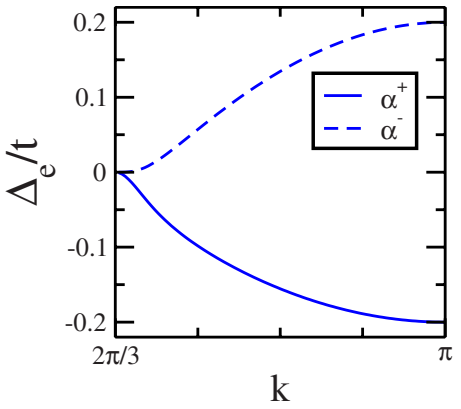

FIG. 4. (Color online) The splitting $\Delta_e(k)$ caused by the edge interactions on the edge states of an α B-ZGNR is presented. We used $t_\perp = 0.2t$ and $t_{edge} = 0.2$.

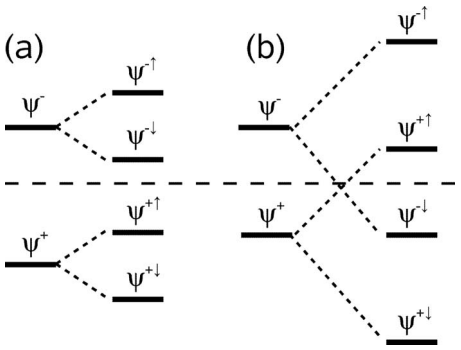

FIG. 5. Schematic scheme of the two situations that can occur if the edge interactions and the magnetism are considered simultaneously. The situation showed in (a) is nonmagnetic. The situation showed in (b) possesses a finite magnetic moment at the edge atoms.

interaction operator annihilates an electron at the site $n=0$ of one layer, and creates an electron at the same site of the other layer. Because of this fact, it is convenient to use the ligand $(\gamma^+ = 1/\sqrt{2}[\gamma^1 + \gamma^2])$ and the antiligand $(\gamma^- = 1/\sqrt{2}[\gamma^1 - \gamma^2])$ states constructed from the eigenstates of Eqs. (24) and (25). The two indexes that define the ligand state for a given k are

$$\gamma_1^+(k,n) = \frac{1}{\sqrt{2}}[C_1^\alpha(k)e^{-ik/2n}D_k^n]$$

$$\gamma_2^+(k,n) = \frac{e^{-ik/2n}D_k^n}{\sqrt{2}}\left[C_2(k) - C_1^\alpha(k)\frac{t_\perp}{t}\left(n - \frac{D_k^2}{1-D_k^2}\right)\right]. \tag{32}$$

The splitting caused by the edge interactions for the above state $(\Delta_e^+ = \langle\gamma^+|H_{edge}|\gamma^+\rangle)$ is given by

$$\Delta_e^+(k) = -t_{edge}C_1^\alpha(k)\left[C_2(k) + C_1^\alpha(k)\left(\frac{t_\perp}{t}\right)\frac{D_k^2}{1-D_k^2}\right]. \tag{33}$$

The antiligand state for a given k is

$$\gamma_1^-(k,n) = \frac{1}{\sqrt{2}}[C_1^\alpha(k)e^{-ik/2n}D_k^n],$$

$$\gamma_2^-(k,n) = \frac{e^{-ikn/2}D_k^n}{\sqrt{2}}\left[C_2(k) + C_1^\alpha(k)\frac{t_\perp}{t}\left(n - \frac{D_k^2}{1-D_k^2}\right)\right], \tag{34}$$

and this state splits as

$$\Delta_e^-(k) = t_{edge}C_1^\alpha(k)\left[C_2(k) - C_1^\alpha(k)\left(\frac{t_\perp}{t}\right)\frac{D_k^2}{1-D_k^2}\right]. \tag{35}$$

In Fig. 4, we show the graphs for the splittings given by Eqs. (33) and (35). The first thing to note is that the electron-hole symmetry is broken. The necessary condition to have an electron-hole symmetry is that the density generated from the occupied states is equal to those generated from the unoccupied states. This occurs when $t_{edge}=0$ because the ligand and the antiligand states, which have different densities, are half-filled and degenerated. But, when $t_{edge}>0$, the splitting leads to a situation where the ligand state is occupied and the antiligand state is unoccupied, and therefore, the electron-hole symmetry is broken.

From Eqs. (33) and (35), we can see that the gap at the first Brillouin border $(k=\pi)$ is exactly $2t_{edge}$ for the α alignment.

When the zero-energy levels are splitted due to the edge interactions, they are still degenerated with respect to the spin degrees of freedown. This degeneracy can be broken if the system becomes magnetized, which can still occur due to a magnetic splitting caused by the Hubbard term. Note that as opposed to the β alignment where such an edge interaction (t_{edge}) is not present and thus any finite value of U leads to a local magnetization, in the α alignment this nonzero value of t_{edge}, and the consequent appearance of a small band dispersion, now requires a critical value of U for the system to become magnetic, as will be shown below. Considering the ligand and antiligand wave functions, the Hubbard contribution from Eq. (28) causes a magnetic splitting given by

$$\Delta_U^+(k) = U\delta[|\gamma_1^+(k,0)|^2 + |\gamma_2^+(k,0)|^2],$$

$$\Delta_U^-(k) = U\delta[|\gamma_1^-(k,0)|^2 + |\gamma_2^-(k,0)|^2], \tag{36}$$

where, $\Delta_U^{+,-}(k) = \langle\gamma^{+,-}|H_U|\gamma^{+,-}\rangle$. The above expressions consider a ferromagnetic configuration. The occurrence of both splittings $\Delta_e(k)$ and $\Delta_U(k)$ simultaneously can result in two distinct situations, shown schematically in Fig. 5.

Situation (i), where the magnetic splitting $\Delta_U^+(k)$ is small, is shown in Fig. 5(a). In this case, the bands for both spin channels associated with the ligand states remain occupied, and the bands for both spin channels associated with the antiligand states remain unoccupied.

In situation (ii) the magnetic splitting is large enough to invert the relative position of the ligand and antiligand bands for one of the spin channels. This situation is shown in Fig. 5(b), and results in a configuration where one ligand band and one antiligand band are occupied for one spin channel, and unoccupied for the other.

To understand when either situation (i) or situation (ii) occurs, let us take the Hartree-Fock total energy, considering that the only bands that vary with δ are those related to the edge states. For situation (i), we have

$$E(\delta) = \frac{1}{\pi}\int_{2\pi/3}^{\pi} dk[\Delta_e^+(k) + \Delta_U^+(k)] + \frac{1}{\pi}\int_{2\pi/3}^{\pi} dk[\Delta_e^+(k) - \Delta_U^+(k)] + U\delta^2 + C. \quad (37)$$

Here, the constant C includes the integral over the nonedge occupied states and the integral over the occupied edge bands from $k=0$ to $k=2\pi/3$. Since the term Δ_U^+ vanishes in Eq. (37), and the term Δ_e^+ does not depend on δ, the integrals in Eq. (37) do not depend on the δ, and the energy minimization condition $dE(\delta)/d\delta=0$ leads to $\delta=0$. This means that the minimum-energy configuration in situation (i) is nonmagnetic.

For situation (ii), the Hartree-Fock total energy is given by

$$E(\delta) = \frac{1}{\pi}\int_{2\pi/3}^{\pi} dk[\Delta_e^+(k) - \Delta_U^+(k)] + \frac{1}{\pi}\int_{2\pi/3}^{\pi} dk[\Delta_e^-(k) - \Delta_U^-(k)] + U\delta^2 + C. \quad (38)$$

and, using Eq. (36) it can be shown that the minimization of the total energy leads to

$$\delta = \frac{1}{2\pi}\int_{2\pi/3}^{\pi} [|\gamma_1^+(k,0)|^2 + |\gamma_2^+(k,0)|^2 + |\gamma_1^-(k,0)|^2 + |\gamma_2^-(k,0)|^2]. \quad (39)$$

The numerical evaluation of the above expression for $t_\perp = 0.2t$ gives $\delta \approx 0.2$. This means that the minimum-energy configuration has a finite local magnetic moment at the edge atoms in situation (ii).

The nonmagnetic configuration (i) occurs until U becomes large enough to turn the configuration (ii) energetically favorable. As a consequence, the system becomes magnetic. Therefore, our analytical model predicts a critical value $U=U_c$, above which the system becomes magnetic. The condition for situation (ii) to be energetically favorable can be calculated by subtracting Eq. (37) with $\delta=0$ from Eq. (38) with $\delta \neq 0$ and imposing that this energy difference is negative. This condition leads to the following expression:

$$\frac{1}{\pi}\int_{2\pi/3}^{\pi} dk[\Delta_e^-(k) - \Delta_e^+(k) - \Delta_U^-(k) - \Delta_U^+(k)] + U\delta^2 < 0. \quad (40)$$

Using Eqs. (36) and (39), the U_c is calculated as

$$U_c = \frac{1}{\delta^2\pi}\int_{2\pi/3}^{\pi} dk[\Delta_e^-(k) - \Delta_e^+(k)]. \quad (41)$$

In particular, for $t_\perp = 0.2t$, and considering Eqs. (33) and (35), the critical value U_c can be calculated by a numerical integration, and is given by

$$U_c = 10t_{edge}. \quad (42)$$

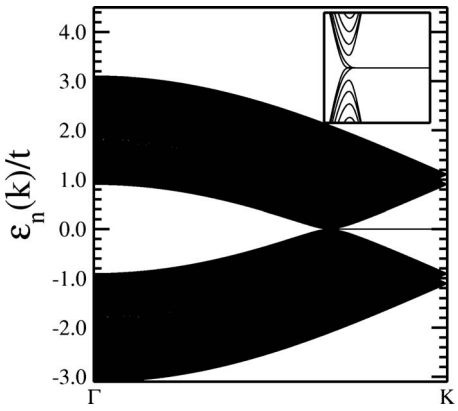

FIG. 6. Energy bands in the regime $U=0$ and $t_{edge}=0$ for $N=100$. There are no differences between the α and the β alignments. At the inset we show in detail the region around the energy zero, limiting the energy axes from $-0.1t$ to $0.1t$, and $k/2=0.29\pi$ to 0.5π.

Because we use first-order perturbation theory, the approximations we made are suitable only for small values of U. In this regime, we found a constant value for δ as well as a linear dependence between t_{edge} and U_c. For large values of U we expect that the nonedge atoms will also be magnetized and the local magnetization will depend on U.

B. Numerical analysis

The analytical analysis presented in the previous section is very useful to understand the main physical characteristics of B-ZGNRs. However, a numerical analysis can be important to take into account other features of the system, such as magnetization of nonedge atoms and properties calculated beyond the first-order perturbation theory. In this section, we will present results obtained from the numerical diagonalization of the Hamiltonian within the Unrestricted Hartree-Fock approximation, showing how the increase of U affects the system.

In Fig. 6 the energy bands for the α alignment in the regime that $U=0$ and $t_{edge}=0$ are presented. Because in this regime the edge states have an energy eigenvalue equal to zero, the energy bands will not depend on the alignment. But, as we have shown, the wave functions differ between the α and β alignments, and when $U>0$ and/or $t_{edge}>0$, many properties will depend on the kind of alignment.

In Fig. 7 the bands for a more realistic situation are presented. Considering $U=t$ and $t_\perp=0.2t$, we show in: (a) the bands for the α alignment with $t_{edge}=0.2t$; (b) the inset for the same bands, where, the solid (blue) lines come from the numerical calculations, and the dashed (red) lines come from the analytical expression [Eqs. (33) and (35)]; (c) the bands for the β alignment with $t_{edge}=0$; A magnified view of the bands in (c) around the energy zero is presented in (d). The solid (blue) lines come from the numerical calculations, and the dashed (red) lines come from the analytical expressions [Eqs. (30) and (31)].

The Figs. 7(b) and 7(d) show that the numerical and the analytical solutions agree very well even for $U \approx t$. The small differences appear mainly because the numerical solution

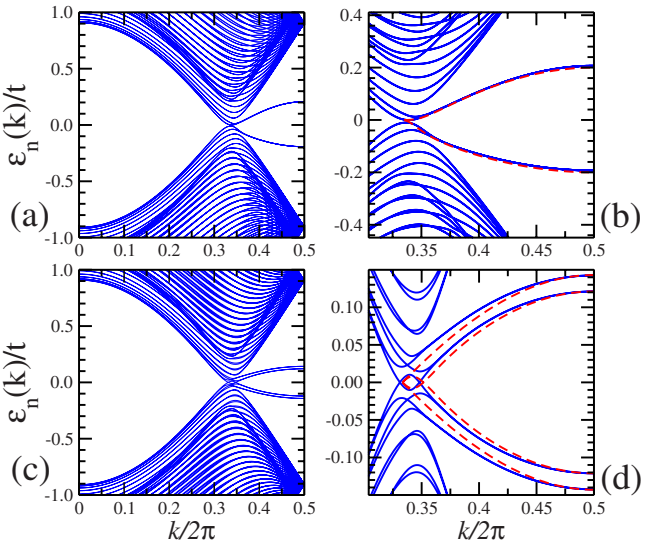

FIG. 7. (Color online) Energy bands for the most realistic situation. In (a) the bands for the α alignment calculated numerically is presented. We used $U=t$, $t_\perp=0.2t$ and $t_{edge}=0.2t$. In (b) the inset of (a) is presented, where the solid (blue) lines come from the numerical solution, whereas the dashed (red) lines come from the analytical expressions of Eqs. (33) and (35). In (c) the bands for the β alignment calculated numerically with $U=t$, $t_\perp=0.2t$, and $t_{edge}=0$ are presented. Here, an antiferromagnetic order is imposed. In (d) is presented the inset of (c), where the solid (blue) lines come from the numerical solution, and the dashed (red) lines come from the analytical expressions of Eq. (30) and (31).

was laterally confined ($N=50$), and because the Hubbard term was simplified in the analytical analysis.

For the beta alignment, the system is always magnetic for $U>0$. For the particular case shown in Fig. 7(c), the edge atoms have a local magnetic moment of 0.3 μ_B. On the other hand, for the α alignment, a nonmagnetic ground state can be found despite the presence of the Hubbard term ($U>0$), as shown in Figs. 7(a) and 7(b). In fact, the presence of the edge magnetization depends on the strength of t_{edge}, and the system becomes magnetic only if $U>U_c$. In Fig. 8 we show the calculated values of U_c, obtained from the numerical diagonalization of the Hamiltonian, which is compared to the analytical expression calculated in the previous section [Eq. (42)]. The linear dependence between U_c and t_{edge} is a good approximation only for small values of t_{edge}, as was expected because it was obtained via first-order perturbation theory.

In order to validate our results in the sense of a more realistic analysis, we compare the bands with the methodology of the present work with the bands calculated with an *ab initio* method based on density functional theory (DFT). Because the interaction between the two layers have a strong contribution from the van der Waals (vdW) interaction, and because the majority of exchange-correlation functionals in use today do not correctly describe the vdW dispersion, we compare our results with those of Ref. 24, which uses a van der Waals dispersion corrected method. The results are presented in Fig. 9 for $N=8$. In (a), we present the bands calculated numerically with the tight-binding method, as obtained in this work, and in (b) we present a DFT calculation, in both cases for the α alignment. The bands in (a) and (b) show that

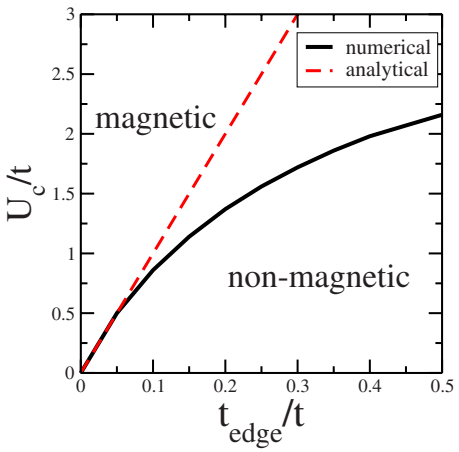

FIG. 8. (Color online) Dependence of U_c with t_{edge}. We used $t_\perp=0.2t$. The solid (black) line was calculated from the numerical solution, and the dashed (red) line is the analytical expression of Eq. (42), which is a good approximation when t_{edge} is small. If $U>U_c$, the system becomes magnetized, while $U<U_c$ leads to a demagnetized solution.

the fundamental behavior is equally described by both methodologies. In both (a) and (b), we found a nonmagnetic state with a finite gap. The energy bands are very similar, and the small differences are related to the edge distortions that occur in the DFT calculation.

In Figs. 9(c) and 9(d), we present the simulations for the β alignment using the methodology of the present work and DFT, respectively. Both calculations agree very well, and predict a magnetic state with a local magnetization at the edge atoms of 0.3 μ_B.

With a mechanism that changes the value of U/t or t_{edge} it is possible to magnetize or demagnetize the α-B-ZGNRs. In

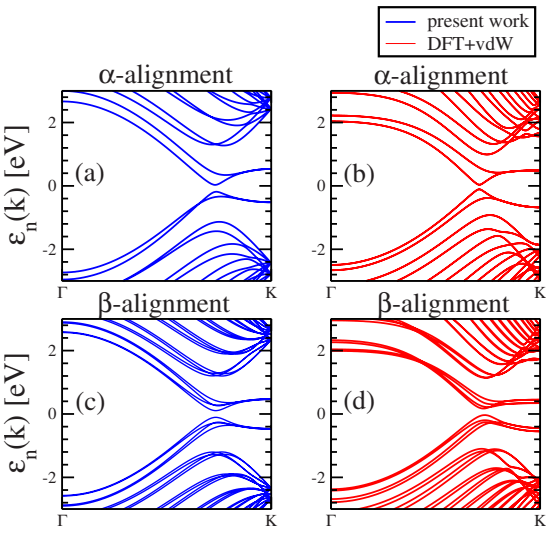

FIG. 9. (Color online) Bands calculated with the methodology of this work compared with first-principles calculations with DFT. The parameters we use are $N=8$, $U=1.3t$, $t_\perp=0.13t$, $t_{edge}=0.2t$, and $t=2.6$ eV. The DFT calculations are performed with the methodology of Ref. 24, which use the PBE(GGA) and include a van der Waals correction. (a) present work, α alignment. (b) DFT, α alignment. (c) Present work, β alignment. (d) DFT, β alignment.

particular, the application of a strain will reduce the hopping t and increase the ratio U/t, favoring the magnetic state. On the other hand, the strength of t_{edge} can be controlled by changing the distance between the edge atoms of the two layers. In particular, applying a pressure near the edges will increase the strength of t_{edge}, favoring the nonmagnetic state.

IV. CONCLUSION

We have investigated the electronic structure and the edge magnetism of Graphene bilayer ribbons using a tight-binding approach. The Hamiltonian we use is composed by a first neighbor hopping along each single layer, interlayer interaction terms, a single-site electron repulsive term via the Hubbard model and an edge interaction term. Two edge alignments are considered: one labeled α, where the outermost atoms of one layer possess one nearest neighbor at the other layer, and another labeled β, where the outermost atoms of one layer possess three nearest neighbors at the other layer.

Through an analytical analysis, we show the differences between these two edge alignments. There are only small differences for the wave function, but the behavior differs qualitatively because of the Hamiltonian symmetry. For the β alignment, the edge atoms interactions are not relevant, and the system becomes magnetic for any $U>0$. For the α alignment, the presence of edge interactions is fundamental to describe a realistic situation. We predict a critical value $U=U_c$, above which the system becomes magnetic. This occurs because there is a competition between a nonmagnetic and a magnetic configuration, and the latter one is energetically favorable only for $U>U_c$. The analytical analysis we made is valid only for small values of U. Therefore, we also present numerical calculations which better describe the regime of larger values of U within the Unrestricted Hartree-Fock approximation. The validation of our results are made by comparing the results obtained with the methodology presented in this paper with *ab initio* calculations. The overall agreement is very good.

Summarizing, the results presented in this work allow us to understand the most fundamental behavior of the magnetism and electronic structure of graphene bilayer nanoribbons with zigzag edge terminations. We suggest that in such systems, the magnetism for the α alignment can be controlled by the application of either strain or pressure.

ACKNOWLEDGMENTS

We thank T. B. Martins for useful discussions, and we acknowledge the financial support from FAPESP and CNPq.

*mplima@if.usp.br
†ajrsilva@if.usp.br
‡fazzio@if.usp.br

[1] J. Chen, M. A. Reed, A. M. Rawlett, and J. M. Tour, Science **286**, 1550 (1999).
[2] Y. Cui and C. M. Lieber, Science **291**, 851 (2001).
[3] J. Li, C. Papadopoulos, J. M. Xu, and M. Moskovits, Appl. Phys. Lett. **75**, 367 (1999).
[4] P. S. Peercy, Nature (London) **406**, 1023 (2000).
[5] R. R. Schaller, IEEE Spectrum **34**, 52 (1997).
[6] Y. Ohno, D. K. Young, B. Beschoten, F. Matsukura, H. Ohno, and D. D. Awschalom, Nature (London) **402**, 790 (1999).
[7] Y. W. Son, M. L. Cohen, and S. G. Louie, Nature (London) **444**, 347 (2006).
[8] K. S. Novoselov, A. K. Geim, S. V. Morozov, D. Jiang, Y. Zhang, S. V. Dubonos, I. V. Grigorieva, and A. A. Firsov, Science **306**, 666 (2004).
[9] K. S. Novoselov, Z. Jiang, Y. Zhang, S. V. Morozov, H. L. Stormer, U. Zeitler, J. C. Maan, G. S. Boebinger, P. Kim, and A. K. Geim, Nature (London) **438**, 197 (2005); Y. B. Zhang, Y. W. Tan, H. L. Stormer, and P. Kim, *ibid.* **438**, 201 (2005).
[10] A. H. Castro Neto, F. Guinea, N. M. R. Peres, K. S. Novoselov, and A. K. Geim, Rev. Mod. Phys. **81**, 109 (2009).
[11] K. S. Novoselov, Z. Jiang, Y. Zhang, S. V. Morozov, H. L. Stormer, U. Zeitler, J. C. Maan, G. S. Boebinger, P. Kim, and A. K. Geim, Science **315**, 1379 (2007).
[12] C. L. Kane and E. J. Mele, Phys. Rev. Lett. **95**, 226801 (2005).
[13] M. Y. Han, B. Ozyilmaz, Y. B. Zhang, and P. Kim, Phys. Rev. Lett. **98**, 206805 (2007).
[14] X. L. Li, X. R. Wang, L. Zhang, S. W. Lee, and H. J. Dai, Science **319**, 1229 (2008).
[15] M. Fujita, K. Wakabayashi, K. Nakada, and K. Kusakabe, J. Phys. Soc. Jpn. **65**, 1920 (1996).
[16] T. Enoki, Y. Kobayashi, and Ken-Ichi Fukui, Int. Rev. Phys. Chem. **26**, 609 (2007).
[17] S. Entani, S. Ikeda, M. Kiguchi, K. Saiki, G. Yoshikawa, I. Nakai, H. Kondoh, and T. Ohta, Appl. Phys. Lett. **88**, 153126 (2006).
[18] H. Min, B. Sahu, S. K. Banerjee, and A. H. MacDonald, Phys. Rev. B **75**, 155115 (2007).
[19] T. Ohta, A. Bostwick, T. Seyller, K. Horn, and E. Rotenberg, Science **313**, 951 (2006).
[20] J. B. Oostinga, H. B. Heersche, X. L. Liu, A. F. Morpurgo, and L. M. K. Vandersypen, Nature Mater. **7**, 151 (2008).
[21] Y. M. Lin and P. Avouris, Nano Lett. **8**, 2119 (2008).
[22] X. R. Wang, Y. J. Ouyang, X. L. Li, H. L. Wang, J. Guo, and H. J. Dai, Phys. Rev. Lett. **100**, 206803 (2008).
[23] B. Sahu, H. Min, A. H. MacDonald, and S. K. Banerjee, Phys. Rev. B **78**, 045404 (2008).
[24] M. P. Lima, A. Fazzio, and A. J. R. da Silva, Phys. Rev. B **79**, 153401 (2009).
[25] K.-T. Lam and G. Liang, Appl. Phys. Lett. **92**, 223106 (2008).
[26] E. V. Castro, N. M. R. Peres, J. M. B. Lopes dos Santos, A. H. Castro Neto, and F. Guinea, Phys. Rev. Lett. **100**, 026802 (2008).
[27] K. Harigaya and T. Enoki, Chem. Phys. Lett. **351**, 128 (2002).
[28] S. Reich, J. Maultzsch, C. Thomsen, and P. Ordejón, Phys. Rev. B **66**, 035412 (2002).
[29] J.-W. Rhim K. Moon, J. Phys.: Condens. Matter **20**, 365202 (2008).

[30] M. P. Lima and G. M. e Silva, Phys. Rev. B **74**, 224304 (2006).
[31] E. V. Castro, N. M. R. Peres, and J. M. B. Lopes dos Santos, J. Optoelectron. Adv. Mat. **10**, 1716 (2008).
[32] T. B. Martins, R. H. Miwa, A. J. R. da Silva, and A. Fazzio, Phys. Rev. Lett. **98**, 196803 (2007).
[33] It has been previously shown (Ref. 34) that for the bulk it is necessary a value of $U/t \simeq 2.23$ for the appearance of a local magnetic moment whereas the real value for this ratio is $U/t \simeq 1.0$.
[34] S. Sorella and E. Tosati, Europhys. Lett. **19**, 699 (1992).